DESIGN AND ANALYSIS OF A NOVEL MEMS-HEAT ENGINE FOR POWER GENERATION

Till Huesgen, and Peter Woias
Department of Microsystems Engineering (IMTEK),
University of Freiburg, Freiburg, Germany

Abstract: A novel self-oscillating micro heat engine for thermal energy harvesting is presented. Its operation principle is based on a cavity filled with a working fluid that performs a self-controlled reciprocating motion between a heat source and a heat sink. A bistable buckling membrane generates the respective upward and downward driving forces upon expansion and contraction of the working fluid. For prediction of the engine performance a lumped parameter system model is developed. A mechanical output power of 0.796 µW is calculated for this first generation device. Test structures were fabricated as silicon wafer stacks to verify the system model. The maximum operation frequency found in the experiments is 1.5 Hz at a temperature difference of 100 K.

Keywords: micro heat engine, bistable membrane, energy harvesting

INTRODUCTION

Distributed sensor networks are a key technology for future smart systems. Despite the broad availability of wireless data communication units, the energy supply of autonomous sensor nodes remains a challenge. Instead of a wire-bound power grid or batteries, micro-scale energy harvesters could provide a flexible solution with virtually unlimited lifetime. These devices are capable of converting ambient energy, often available as waste heat, into useful electrical energy. On microscale, thermal energy is commonly harvested by thermoelectric generators, based on the Seebeck effect [1]. However, these generators show inherently low efficiencies. On a macroscopic scale, thermodynamic heat engines, such as Stirling engines or steam turbines, show considerably higher efficiencies, due to the thermodynamic cycle involved. The direct miniaturization of these complex devices, however, has proven to be problematic, due to unfavorable scaling laws. At Washington State University, a new type of micro-scale heat engine with a membrane setup instead of a piston was developed [2]. Alternated heating and cooling of a working fluid causes the membrane to oscillate. The major drawback of this concept is the need for an active control of the thermal switch, which of course requires energy itself [3]. Song et al. proposed a thermal oscillator based on a bistable membrane [4]. A centimeter-sized functional demonstrator with an oscillation period of 70 sec was built as prove of principle.

This paper presents a self-starting and self-regulating chip-scale heat engine based on the work of Song et al. A schematic cross-sectional view of the micro heat engine is shown in Fig. 1. A cavity is formed by a rigid plate on top and a bistable membrane on the bottom side. Due to mechanical pre-stress, the bistable membrane is either bulged into the cavity or out of the cavity. The cavity is filled with a working fluid, either a gas or a liquid-gas phase-change medium. This unit, called engine chamber, is mechanically fixed to a heat source with a thermally insulating post, located in the middle of the membrane. On top, a heat sink is separated by an air gap from the engine chamber. In operation, as illustrated in Fig. 2 a) and b), heat flows through the thermal interface between the heat source and the body of the engine chamber to the working fluid. Hence, the interior pressure rises. When the threshold pressure is exceeded, the membrane snaps outwards, lifting the entire engine chamber until it gets in contact with the heat sink. Heat is transferred out of the engine chamber and the working fluid pressure decreases. Eventually, the pressure falls below the negative threshold, causing the membrane to snap inwards and the engine chamber moves down again.

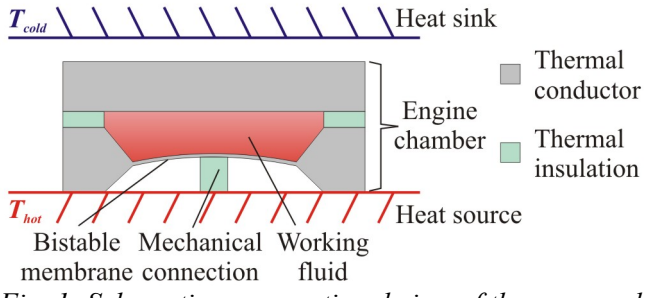

Fig. 1: Schematic cross sectional view of the proposed micro heat engine.

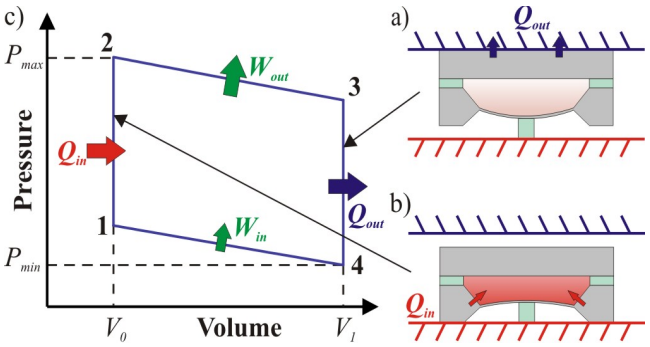

Fig. 2: a) Schematic of the engine during cooling in the upward position, b) during heating in the downward position and c) p-V diagram of the cycle: isochoric heating 1-2, adiabatic expansion 2-3, isochoric heat rejection 3-4, and adiabatic compression 4-1.

Thereby, the working fluid undergoes a thermodynamic cycle which can be approximated by ideal isochoric and adiabatic state transitions as shown in Fig 2 c).

In the following theory section, the membrane mechanics is analyzed. The thermodynamic cycle of an engine with air as working fluid is presented. These results are applied to develop a system level model of the engine. The experimental section details the fabrication of a functional demonstrator as well as its testing. The results prove the feasibility of the concept.

THEORY

Bistable Membrane

Bistable Si membranes are fabricated by compressive prestressing with an SiO_2 layer [5,6]. When the energy due to deformation of the middle plane, caused by the compressive pre-stress, becomes larger than the strain energy of bending, buckling occurs. When such a buckled membrane is subjected to a transversal differential pressure, it shows a hysteresis behavior as shown in Fig. 3. For the engine design, two properties are of major importance: First, the threshold pressures, at which the membrane is switched upwards and downwards, and second, the displacement volume, which is a function of the membrane center deflection. These properties are determined by 3D FEM simulations with ANSYS. In this paper square-sized composite membranes from 8 µm Si and 2 µm SiO_2 and with an edge length of 3 mm are considered. The simulated volume displacement is $\pm 1.3\times10^{-10}$ m^3 at threshold pressures of ±4900 Pa. These results were experimentally verified as shown in Fig. 3.

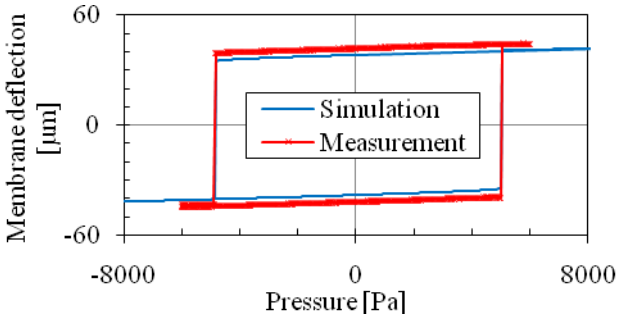

Fig. 3: FEM simulation results and measurement data for the pressure-dependent membrane center deflection of square Si/SiO_2 (8 µm/2 µm) membrane with 3.0 mm a edge length.

Thermodynamic Cycle

The thermodynamic cycle of the engine with air as working fluid is analytically modeled under several assumptions:

- Ideal gas law applies for the working fluid.
- The gas is spatially isothermal.
- The membrane is treated as an ideal bistable membrane, thus heating and cooling are isochoric process.
- The expansion and compression of the working fluid are adiabatic processes, due to the fast snapping motion of the membrane.

The calculation of the state properties during the thermodynamic cycle is performed using the ideal gas law and the equation for adiabatic state transitions:

$$pV = nRT$$

$$p_1 V_1^{\kappa} = p_0 V_0^{\kappa}$$

where R is the ideal gas constant, n the amount of gas, p the pressure, V the fluid volume, and κ the isentropic coefficient.

Table 1 shows the calculated results for the thermodynamic cycle as presented in Fig 2 c) for an engine design with a cavity volume of 1.14×10^{-8} m^3, which has been sealed at an ambient pressure of 992 hPa and a temperature of 330 K. The mechanical work output per cycle is 1.91 µJ and the cycle efficiency is 10.98 % of the Carnot efficiency.

Table 1: Calculated thermodynamic cycle of the heat engine with states as shown in Fig. 2 c).

Step	Temperature [K]	Pressure [Pa]	Volume [$\times10^{-8}$ Pa]
1	320.7	96 409	1.131
2	346.3	104 100	1.131
3	344.1	101 805	1.494
4	318.7	94 300	1.494

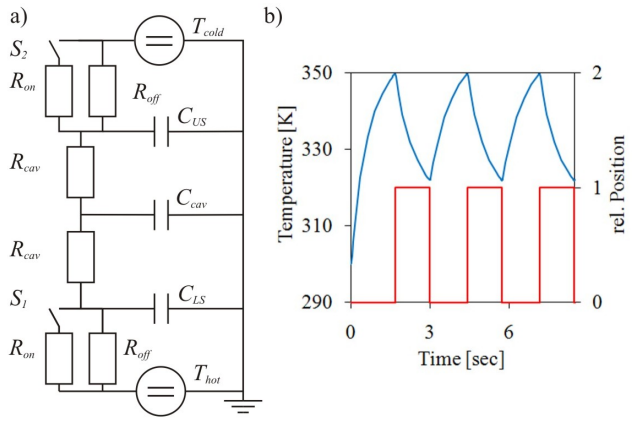

Fig. 4: a) Lumped parameter model for a transient thermal analysis. b) Simulation results showing the cavity temperature and position as a function of time.

Lumped parameter system model

A simple lumped parameter model of the moving cavity as shown in Fig. 4 a) is developed for a transient simulation of the engine operation. Here, heat transport and storage are represented by equivalent resistors and capacitors. The capacitors C_{US}, C_{cav}, and C_{LS} denote to the heat capacity of the upper substrate, the cavity, and the lower substrate, respectively. The cavity thermal resistivity is represented by R_{cav}, whereas the interface thermal resistivity is R_{on}, when the engine chamber is in contact, and R_{off} if not. Due to the high thermal conductivity of the silicon, the thermal resistance of the substrates can be neglected. The switches S_1 and S_2 are switched alternately to simulate the cavity being in contact either with the heat source or with the heat sink. Fig. 4 b) shows the simulated working fluid temperature and cavity position for a first, non-optimized, design. This engine has a membrane size of 3.0×3.0 mm² and air as working fluid, as detailed above. The simulated cycle time is 2.4 sec, which yields a theoretical mechanical power output of 0.796 µW.

DEVICE FABRICATION

The fabrication of the device involves four 100 mm silicon wafers as illustrated in Fig. 5. Wafer one, 375 µm thick, forms the cap of the engine chamber. A sandwich of thermal SiO_2 and LPCVD Si_3N_4, 300 nm and 100 nm thick, serves as temporary masking material for the backside fluidic via formation with KOH. On the front side 90 µm of Ordyl, a permanent dry-film photoresist, are laminated and structured by photolithography. Besides the formation of the cavity, the Ordyl also serves as thermal insulation and bonding layer. The second wafer, 500 µm thick, forms the bottom of the engine chamber with the bistable membrane. For pre-stressing of the membrane, 1000 nm thermal SiO_2 and 1000 nm low frequency PECVD SiO_2 are deposited with an average compressive stress of 300 MPa. KOH wet etching is used to release the membrane sandwich composed of 8 µm Si and 2 µm SiO_2. The etch stop is time controlled. Both wafers are aligned and directly bonded by applying heat and pressure. More details on the adhesive bonding process with Ordyl are given elsewhere [7].

The heat source and heat sink are formed by two further wafers, each 500 µm thick. For a better thermal insulation, a recess is etched with KOH into the heat source, leaving a protruding central post for the mechanical connector. Around, a gold RTD is structured. The final assembly of the device is carried out on chip-level. Thereto, the engine chamber wafer stack is diced to 9×9 mm² chips, whereas the heat source and heat sink wafers are diced to 14×16 mm² chips. A drop of epoxy is dispensed onto the post in the middle of the heat source chip before the engine chamber is placed on top using a flip-chip bonding tool. In order to achieve a pre-tension, the engine chamber is heated to a temperature just below the threshold, where the membrane would snap outwards. Fig. 6 a) shows an optical micrograph of the engine. The heat sink chip is aligned with an air gap of 60 µm in the measurement setup, as detailed below.

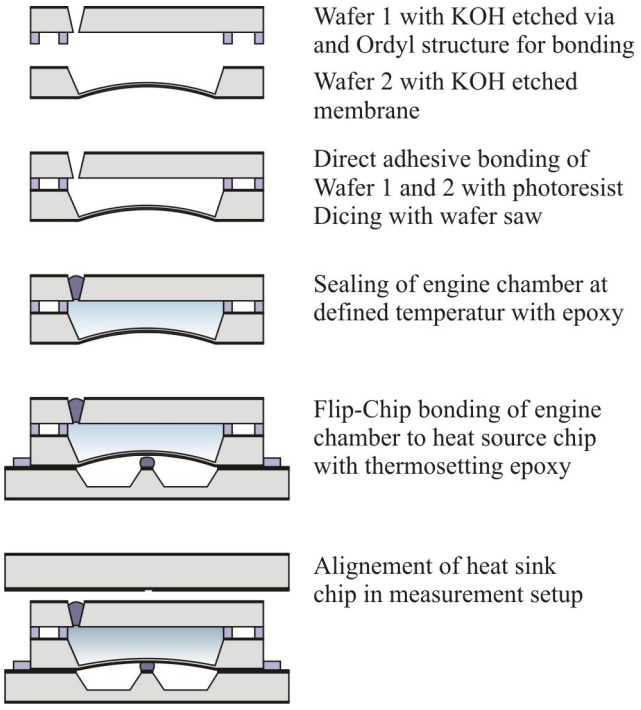

Fig. 5: Schematic outline of the fabrication process of the micro heat engine. The first steps are carried out on wafer-level. Only the final assembly is performed at chip level.

RESULTS

For characterization the device is placed, with its heat source looking up in the measurement setup as shown in Fig 6 b) and c). A manual z-stage is used to adjust the gap between the engine chamber and the cold side chip to approximately 60 µm. The temperature gradient is established by a resistive heater on the hot side and a liquid flow cooling system with an additional Peltier cooler on the cold side.

Measurement results for the operation frequency as a function of the applied temperature difference are shown in Fig. 7. The maximum operation frequency is 1.2 Hz at a temperature difference of 100K. If the gap size is decreased by 10 µm during operation, the operation frequency increases to 1.5 Hz.

In order to determine the maximum stroke, the engine is placed on a thermochuck. A laser distance sensor records the cavity position as a function of temperature. It was found that the stroke of the cavity is 80 µm between the downward position at room temperature and the upward position at 90°C.

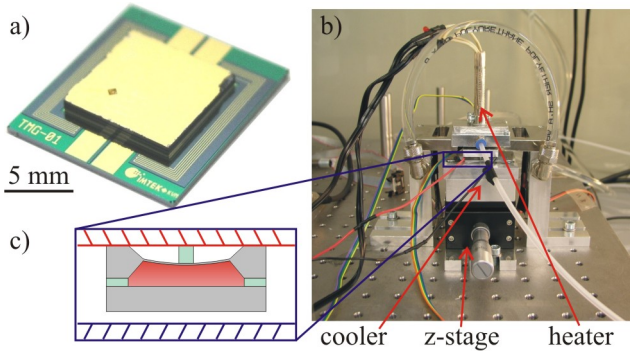

Fig. 6: a) Optical micrograph of the device, b) Photograph of the measurement setup, and c) schematic close-up view indicating the engine location and orientation.

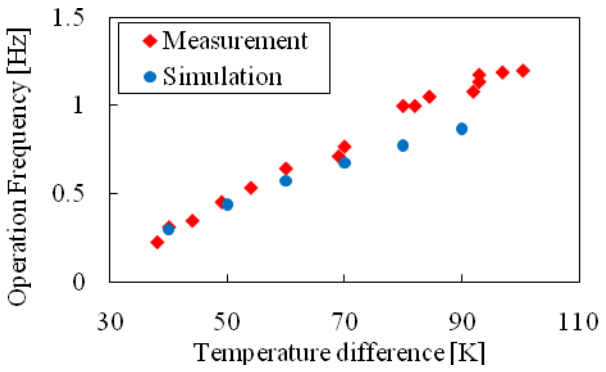

Fig. 7: Measured operation frequency and simulation results as a function of the applied temperature difference.

CONCLUSION

The results presented above demonstrate the feasibility of the concept and the exertion of a complete thermodynamic cycle with sharp phase transitions. The engine is self-starting and self-regulating, as the operation frequency depends on the applied temperature difference. The maximum operation frequency found in the experiments is 1.5 Hz at a temperature difference of 100 K.

So far, air has been theoretically and experimentally investigated as working fluid. Actual research concentrates on the introduction of phase-change fluids. Further, a more advanced functional prototype with an integrated mechano-electric generator is under development.

ACKNOWLEDGEMENTS

The financial support of the Deutsche Forschungsgemeinschaft DFG under the graduate research training program GR1322 “Micro Energy Harvesting” is gratefully acknowledged.

REFERENCES

[1] Hudak N S, Amatucci G G 2008 Small-scale energy harvesting through thermoelectric, vibration, and radiofrequency power conversion *J. Appl. Phys. 103*, 101301

[2] Whalen S, Thompson M, Bahr D, Richards C, Richards R 2003 Design, fabrication and testing of the P3 micro heat engine *Sensors and Actuators A 104* 290-298

[3] Cho J H, Weiss L W, Richards C D, Bahr D F, Richards R F 2006 Power production by a dynamic micro heat engine with integrated thermal switch *Technical Digest PowerMEMS 2006 (Berkley,USA 29 November - 1 December 2006) 9-12*

[4] Song G, Kim K, Lee Y 2007 Simulation and experiments for a phase-change actuator with bistable membrane *Sensors and Actuators A 136* 665-672

[5] Popescu D S, Lammerink T and Elwenspoek M 1994 Buckled Membranes for Microstructures *Proc. IEEE Workshop on Micro Electro Mech. Syst. (Oiso, Japan)* 188–92

[6] Malhaire C, Didiergeorges A, Bouchardy M, Barbier D 2002 Mechanical characterization and reliability study of bistable SiO2/Si membranes for microfluidic applications *Sensors and Actuators A 99* 216-219

[7] Huesgen T, Bartsch U, Albrecht B, Vulto P, Gaspar J, Woias P 2008 Wafer-Level Dry-Film Photoresist Adhesive Bonding For 3D-MEMS Integration and Packaging *Proc. Micromechanics Europe Workshop 2008 (Aachen, Germany 28-30 September 2008)* 255-258